The High-Gain Harmonic-Generation Experiment At the BNL Accelerator Test Facility: A SASE / Seeded FEL Using the Cornell Wiggler

BNL National Synchrotron Light Source
and
Argonne Advanced Photon Source

Motivation

Short wavelength Free-Electron Lasers are perceived as the next generation of synchrotron light sources. In the past decade, significant advances have been made in the theory and technology of high brightness electron beams and single pass FELs. These developments facilitate the construction of practical UV and X-ray FELs and have prompted proposals to the DOE for the construction of such facilities. Self-Amplified Spontaneous Emission (SASE) and High Gain Harmonic Generation (HGHG) are the two leading candidates for VUV to X-ray FELs.

There is a broad-based recognition in the synchrotron light source community that there is user interest and it possible to extend FEL operation to x-rays. The technology that makes this possible is photo-injectors with emittance compensation, transport, acceleration and compression of high brightness beams without emittance dilution, high precision undulators and advances in theory and simulations. In addition short wavelength FELs offer the possibilities of extremely high peak power and very short pulses.

Several groups in the USA are developing plans for such short wavelength FEL facilities. However, reviewers of these plans have pointed out that it would be highly desirable to first carry out proof-of-principle experiments to increase confidence that the shorter wavelength devices will indeed perform as calculated. The FEL community has now broadly accepted the need for such experiments.

The BNL Accelerator Test Facility (ATF) is a logical place to carry out such experiments. It is a user facility dedicated to accelerator and beam physics experiments. It offers a very high brightness electron beam at energies up to 70 MeV, lasers that are synchronized to the electron beam and well-equipped beam lines. The HGHG experiment has been approved by the Steering Committee that guides the ATF and it is scheduled to go onto the beam line in 1997. The availability of the Cornell wiggler (see details below) makes it possible to execute a SASE experiment early in 1997 (see tentative schedule below). The experiment will be implemented on the ATF Beam Line 2, the location of the HGHG experiment. This line has operated with electron beam for a few experiments, including a

10 micron Inverse FEL. It is very well instrumented and includes an entry port for the CO_2 laser.

The experiments that can be done include the study of start-up from noise, verification of the theory for the gain length at wavelengths in the 10 to 5 microns range as well as study of the saturation regime, using the ATF's CO_2 laser for seeding the FEL.

The SASE experiment will be carried out by a collaboration of the NSLS at BNL and the APS at ANL. Following the SASE and seeded beam experiments the HGHG experiment will proceed to the generation of harmonics.

Once the SASE and seeded experiment are carried out, it would be possible to proceed to HGHG experiment with the addition of a dispersion section and a modulator wiggler section. The mini-undulator available at NSLS is a suitable candidate for the modulator wiggler of the HGHG setup.

High Gain Harmonic Generation FEL

Currently there are two possible paths to high-power, single-pass short-wavelength FELs: SASE and HGHG. The HGHG technique seems to offer an order-of-magnitude better bandwidth, a signal free of noise, improved wavelength stability and a shorter wiggler but seems to be limited to longer wavelengths than SASE.

In recent years there has been an enhanced interest in the generation of coherent, short pulse Free-Electron Laser (FEL) radiation. In particular there is interest in single-pass devices, such as Self-Amplified Spontaneous-Emission (SASE). At Brookhaven National Laboratory we have been pursuing a different approach to short wavelength FELs. We call this approach High-Gain Harmonic Generation (HGHG).

In HGHG, a seed laser is used to modulate the energy of an electron beam in a 'modulator' wiggler. The energy modulation is converted to spatial bunching in a dispersive section that follows the modulator. The bunched beam is introduced to a wiggler tuned to the desired harmonic of the seed. The radiation at the harmonic wavelength starts as a coherent spontaneous signal, which quickly changes to exponential regime growth, and, if the wiggler is long enough can reach saturation. Tapering may follow to extract more energy.

FEL Performance Overview

FEL parameters

We expect to operate the SASE FEL in the wavelength range between 5 and 10 microns. The electron beam parameters and wiggler parameters used for the estimate of 5 micrometer operation are given in the table below. The calculations for the power gain length were done analytically, using the 3-D universal scaling law.

PARAMETER	UNITS	VALUE
Electron beam energy	γ	82
Normalized rms emittance	mm-mrad	4
Current	amperes	110
Energy spread (rms, relative)	%	0.044
Bunch length (square pulse)	ps	4.5
Wiggler peak field	Tesla	0.467
Wiggler period	cm	3.3
Wiggler length	m	2
Betatron wavelength	meters	3.76
Power gain length	meters	0.26
Radiation wavelength	micrometers	5

SASE spectral characteristics and requirements of diagnostics

The estimated characteristics of the radiation for 5 microns radiation are presented in the table below. The purpose of these numbers is to guide the experiment regarding the detection of the SASE radiation and the design of the experimental equipment.

PARAMETER	UNITS	SASE	SPONTANEOUS
Power per unit relative bandwidth	Watt	1000	29
Power (including all harmonics)	Watt	-	54
Power in fundamental	Watt	29	9
Central cone:			10^9
Power	Watt	29	0.47
Energy/pulse	pJ	130	2
Photons/pulse	-	3.3×10^9	5×10^7
Bandwidth	%	2.8	1.7
Divergence angle	Radians	3.3×10^{-3}	2.2×10^{-3}

A detailed explanation of the definitions of the quantities given in this table will be given in the theoretical section of this design book. The power per unit relative bandwidth should be measured with an acceptance that is larger than the divergence angle given above. The power in the fundamental is the power integrated over a range of bandwidth and divergence angle larger than those given in the table. The power, energy per pulse, and photons per pulse in the central cone are all referred to the spontaneous radiation in the bandwidth and divergence angle given in the table. The bandwidth given above should be measured using a pin-hole much smaller than the divergence angle of the radiation. The divergence angle given here should be measured with a bandwidth much less than the bandwidth given above. The electron pulse shape is idealized as a flat top square pulse even though the ATF gun simulation indicates that the pulse has a tail comparable to the pulse width itself and may contribute to additional spontaneous radiation.

It is clear from the results that a narrow band detection will signal the SASE results in a much clearer way, since the signature of SASE is more pronounced in the power per unit relative bandwidth than that of the total power. Notice that the bandwidth and the divergence angle for SASE is larger than spontaneous emission contrary to the general impression.

If we increase the wavelength to 10 microns, the signature of SASE even for total power would become more pronounced. The parameters we assumed for the estimate and the results are given in the next table.

Seeded FEL at 5 and 10 microns

With the ATF's CO_2 laser, we can seed the FEL at 10 and 5 microns (the 5 microns seed will be the doubled CO_2). With a seed radiation we can easily reach and study saturation as a function of the seed power. Simulation shows the optimized gain to be 160 at 5 micron. The CO_2 pulse length is about 100 ps. The electron pulse is about 5 ps. Because this mismatch of pulse length, the measured gain should show a factor of 8 instead of 160. At 10 microns the ratio will be better.

PARAMETER	UNITS	SASE	SPONTANEOUS
Electron beam energy	γ	58	58
Normalized rms emittance	mm-mrad	4	4
Current	amperes	110	110
Energy spread (rms, relative)	%	0.044	0.044
Bunch length (square pulse)	ps	4.5	4.5
Wiggler peak field	Tesla	0.467	0.467
Wiggler period	cm	3.3	3.3
Wiggler length	m	2	2
Betatron wavelength	meters	2.66	2.66
Power gain length	meters	0.2	
Radiation wavelength	micrometers	10	10
Power per unit relative bandwidth	Watt	4300	15
Power (including all harmonics)	Watt	-	27
Power in fundamental	Watt	140	4
Central cone:			
Power	Watt	140	0.24
Energy/pulse	pJ	630	1
Photons/pulse	-	3.2×10^{10}	5×10^{7}
Bandwidth	%	3.3	1.7
Divergence angle	Radians	5.3×10^{-3}	3.2×10^{-3}

Wiggler error tolerance

Based on our previous analysis, the wiggler error should be characterized by the electron trajectory rather than the wiggler field error. Using multi-particle simulation with the TDA-3D code we carried out a preliminary study of the gain as a function of the transverse rms displacement of the trajectory. The wiggler field is given by a set of random numbers without correlation (each half period is independent). The error distribution is governed by a field rms error. We assume that there are five beam position monitors, three equally spaced inside the wiggler, and enough beam steerers to position the beam back on axis at each diagnostic. The electron beam is represented by 1200 particles with a quiet start random distribution.

With multiple runs with different random seeds we arrive at the distribution of power vs. Rms trajectory displacement. The computation uses two different sets of wiggler errors. One set has a 1% rms ΔB/B, the other has a 0.5% rms ΔB/B. The first set has a large range of the power distribution, showing that a 1% rms ΔB/B is too large as a general guide but certain random sets of course may be acceptable. However this should not be taken to be the guideline of tolerance decision because half period wiggler error correlation length is not necessarily realistic. On the other hand our analysis and the figure both show that rms trajectory displacement is a good measure of gain reduction. Based on this we conclude that the rms displacement of the electron trajectory in the wiggler should be less than 100 microns. Notice that because the betatron wavelength is comparable to the wiggler length, the focusing effect is important, and the trajectory deviation from a straight line should be used as the tolerance criterion instead of the second field integral.

Electron beam optics and wiggler focusing

Equal focusing along the wiggler

The gain of free-electron laser depends critically on maintaining a precise phase relationship between the wiggle motion and the electric field of the light. It is necessary to effectively control the transverse betatron oscillations of the particles to satisfy this relationship. In a linear wiggler of conventional design, focusing is provided by the wiggler in only one transverse direction (the vertical direction). External focusing, provided by adding a quadrupole component to the field, is required in the other transverse direction (the horizontal plane). The maximum magnetic field in the wiggler required for this experiment is ***B*max=*0.467* T** for an electron beam energy ***E=42 MeV***. This determines the required values of the quadrupole component and transverse beta functions. The equations are as follows.

$$b_x := \left(\frac{e}{P_o}\cdot\frac{dB_y}{dx}\right)^{-\frac{1}{2}}$$

$$b_y := \left[\left(\frac{e}{P_o}\cdot\frac{B_{max}}{\sqrt{2}}\right)^2 - \frac{e}{P_o}\cdot\frac{dB_y}{dx}\right]^{-\frac{1}{2}}$$

The quadrupole component of magnetic field produced by the four wire corrector was calculated with two assumptions. First, the effect of the iron poles is not included, and second, the conductors are assumed to be infinitely thin. The 67.5° angle between the wire and the wiggle plane of the undulator, which initially was determined from requirement for uniform steering, actually provides optimal homogeneous focusing in both the horizontal and vertical planes. The measurement of the quadrupole component of magnetic field was made with a hall probe.

Actually, the surrounding iron in the wiggler can be readily taken into account in the approximation of continuous iron (no space between poles; *m~ ¥*) and where the distance between the conductors and the iron ***(d)*** is much larger than the beam axis to wire distance ***(r)***. In the real system *d*· ***1mm*** and *r~* ***7mm***. It is therefore necessary consider image currents in the iron. This effect approximately doubles the gradient. This was verified experimentally with continuous unsaturated iron surrounding wires. The real result for the Cornell wiggler around the focusing vacuum chamber will differ slightly differ due to real shape of currents and poles. The measured strength in prototype tests for the NISUS undulator was reported to be ***2.7 G/cm/amp.***

Another factor, which must be considered in the real experiment, is that the focusing is not continuous along the full length of the wiggler. Four separate corrector stations each 25.1-cm long are distributed over the wiggler. In effect, the corrector stations occupy half the length of the wiggler, so the required focusing strength from each must be doubled. One can therefore easily estimate that the required current will be:

I=2*(39 G/cm)/(2.7 G/cm/amp) *»* ***30 amps***.

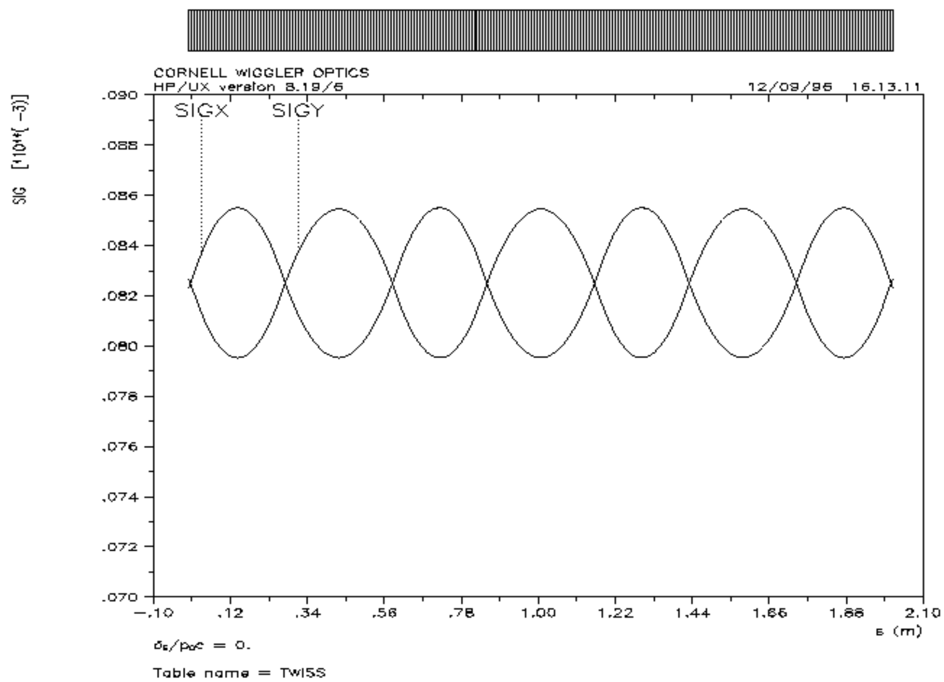

Modulation of beam size in the wiggler.

Beamline 2 transport optics

There are several requirements on the beam transport optics:

1. Correspondence of beta function at the wiggler entrance;
2. Wiggler should be installed as close as possible to the end of line;
3. Zero dispersion function in the line;
4. Small modulation of beta function.

The requirements are satisfied with the present complement of optical elements in the beamline. A transport calculation was made using the MAD code. The wiggler was simulated as a continuous series of rectangular magnets (4 magnets per wiggler period). Some of these magnets have a focusing component while the balance is all pure dipole. The position of both types magnets corresponds to the position of the four correction stations and non-focusing diagnostic sections inside the wiggler. The magnetic field of this array was set to $\mathbf{B}_{\mathbf{max}}$/ö**2**, which corresponds to the real configuration. The beamline 2 elements are presented below in the MAD format:

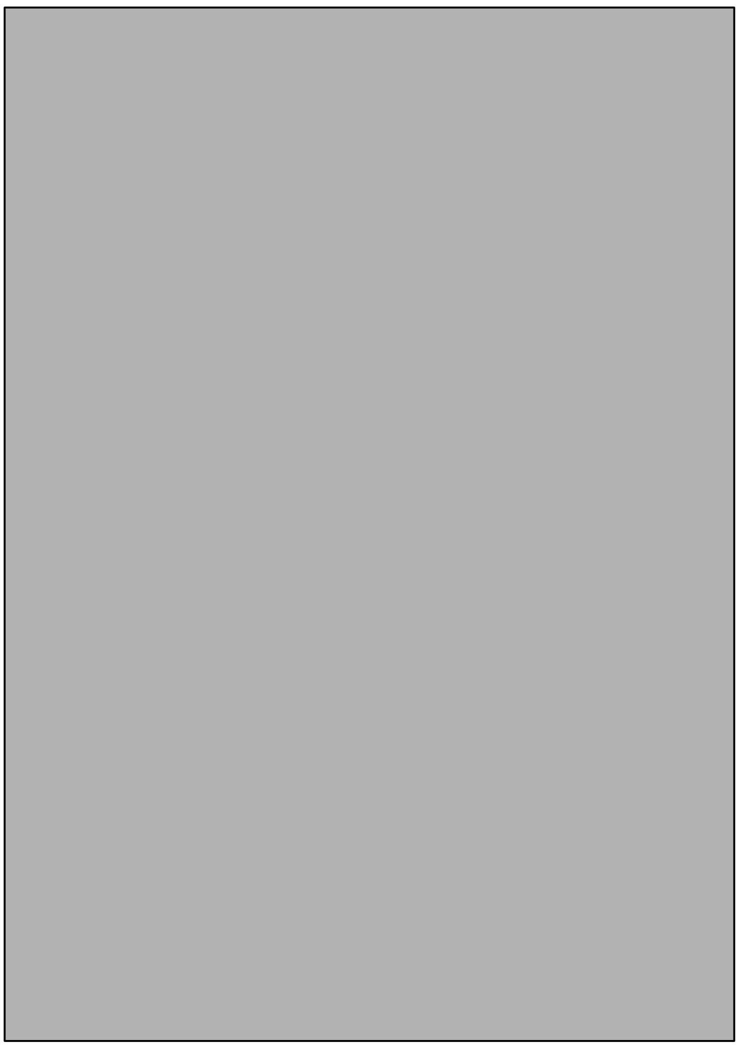

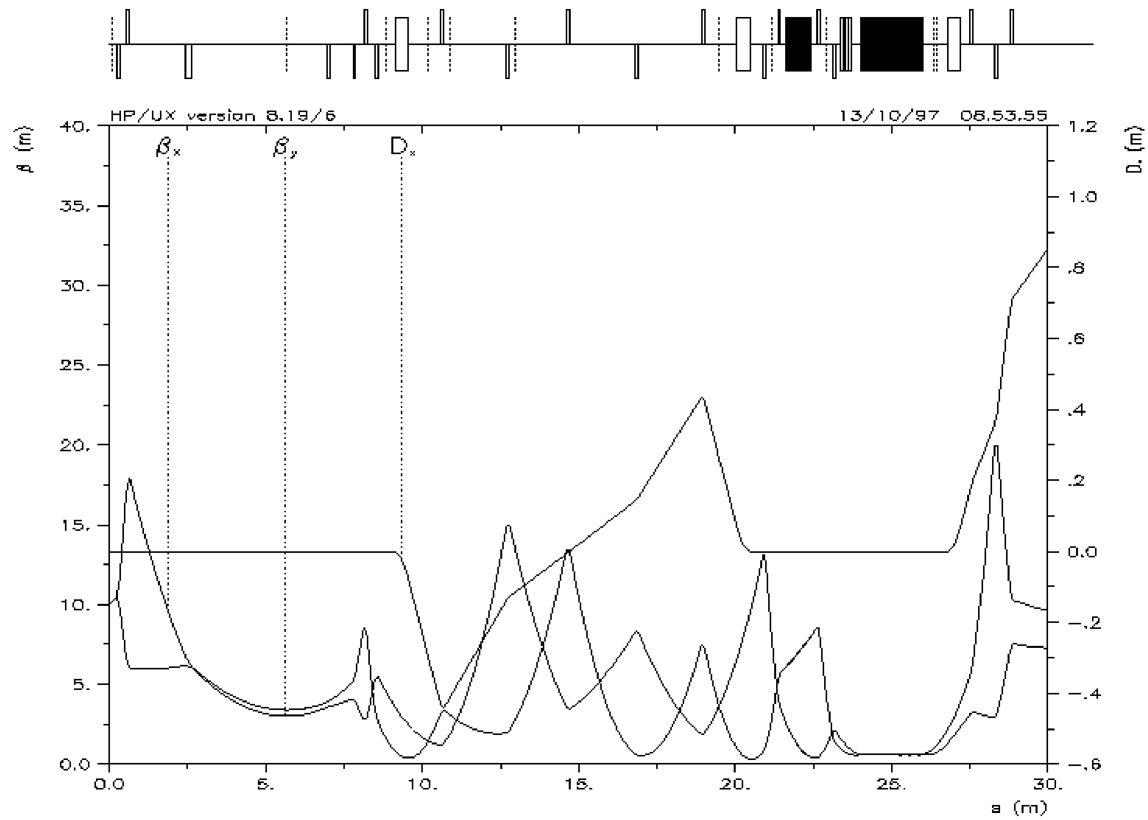

Optical functions for transport into Beamline 2 including the wiggler.

ATF considerations:

Introduction

The ATF's S-band one-and-half cell photocathode RF gun (or photoinjector) is followed by a solenoid magnet used for emittance compensation. A copper cathode has been chosen as the photo-emitter due to its unlimited lifetime at a reasonable vacuum although its quantum efficiency is low. Magnetic measurements were performed to insure that the longitudinal magnetic field on the cathode surface is nearly zero. Following the solenoid magnet is a 45-degree aluminum mirror for monitoring the laser beam profile on the cathode and carrying out optical transition radiation (OTR) measurement. A phosphor coated copper block on an actuator is next in line for charge measurements. This copper block can also be used for beam profile and position monitoring. The beam is then injected into the linac. The distance between the cathode and the entrance of the linac is 81 cm, optimal for emittance compensation. The linac consists of two sections of SLAC type traveling wave linac. The RF gun and linac are powered separately by two XK-5 klystrons.

The ATF's photoinjector and two linac sections are laid out in a straight line with nine quadrupole lenses, numerous steering magnets and many beam position and profile monitors. The quadrupoles are used for beam matching or emittance measurements, utilizing two beam profile monitors with a five-meter separation. A 20° dipole magnet bends the beam into a dispersive section with more magnets and diagnostics, including a momentum analysis slit for energy spread measurement or energy selection. Additional 20° dipoles in this line can bend the beam into three dispersion free beam lines in a shielded experiment hall.

Electron Beam Properties

The ATF energy is continuously variable from about 25 MeV to about 70 MeV. (At the time of writing the maximum energy is 40 MeV due to a bad klystron that is scheduled for replacement in December 1996). The charge is continuously variable from the limit of detectability to 0.5 nC per pulse at the time of writing of this document, with a scheduled upgrade to over 2 nC in December 1996. The electron beam pulse length, its energy spread and its emittance are a function of the laser to RF phase in the gun

ATF Electron beam diagnostics

The main electron beam diagnostic devices at the ATF are Faraday cups, phosphor screen beam profile monitors and strip-line beam position monitors. For electron beam energy measurement, several spectrometers consisting of dipole magnets, quadrupole lenses and beam profile monitors are in use. Transition radiation is used extensively at the ATF for beam energy, transverse beam profile and bunch length measurements. The ATF beam profile monitors comprise an imaging system, motorized or pneumatic insertion control system and image analysis. The imaging system comprises a Gd_2O_2S:Tb phosphor deposited on a one mil thick aluminum foil, an aluminum mirror mounted at 45° and a pair of lenses. The phosphor screen is perpendicular to the electron beam, improving the resolution of the BPM. Two lenses image the electron beam image with a magnification of f1/f2. The focal length f2 is short, resulting a large light collection angle. A motorized aperture on the lens controls the intensity of the image. Our measurement showed that this BPM has a resolution of 50 μm, and a sensitivity of 5 pC with 0.5-mm diameter spot.

The ATF's BPM can be easily converted into an optical transition-radiation beam profile monitor by simply removing the phosphor screen. The CCD cameras currently in use are Pulnix 745E or WAT902A. The later has been used for OTR measurement. A good OTR image is obtained at beam energy of 40 MeV for a charge of 0.25 nC. The BPM was used for transverse emittance measurement, employing both the quadrupole magnet scan and the multiple screen methods.

The ATF beam position monitor consists of a beam pick-up element with four stripline electrodes in a 1.5" diameter stainless steel pipe mounted with 2 3/4" diameter Con-flat flanges, and a local receiver. The electrodes are shorted at the downstream end, resulting a bipolar output signal with a separation of 550 ps, twice the length of the electrode. The signals are converted to unipolar video signals in a balanced mixer driven by a reference. Pass band filters are used to select the desired Fourier component of the bipolar pulses. The current reference frequency is 2856 MHz, which is about the third harmonic in the bipolar signal's spectrum. Currently we are in the process of changing over to a about 1 GHz reference, at which better performing components are available. The video output is amplified and sent to charge sensitive ADCs.

Wiggler Modifications

Mechanical support system

Based on a study for the installation of the Cornell wiggler into the ATF Beamline #2 it is recommended that the existing be replaced by an alternative support system as depicted on the attached figures. This recommendation is based primarily on the implications of the limited space around beamline 2 on the installation and commissioning of the wiggler.
The current stand design would interfere with many of the components on the floor of the ATF experimental hall and would make the magnet installation very difficult. The magnets would have to be located with the only access to the magnet aperture facing west toward beamline 3. This would make access to both the wiggler aperture and the FEL experiment currently in place in beamline 3 very difficult, and provide a serious and unnecessary complication of the design of the Cornell wiggler beam tube and diagnostics section. The legs of the current stand would also be a trip hazard as they would cross the pathway between beamline 2 and beamline 1. This would also hamper access to equipment and experiments up beam from the wiggler on both beamlines.

Any other installation scenario would include the temporary removal of the down beam Danfysik dipole magnet and quadruple diagnostic optics of beamline 2. This scenario threatens the geometric integrity of beamline 2, resulting in significant labor costs and downtime, and should be avoided. In the proposed scenario a supporting frame and strut system is designed to transport and then rigidly support the wiggler assembly.

It is suggested that adapter plates be fabricated and affixed to the sides of the two support columns. Holes and slots in the sides of the wiggler support column as depicted in Spectra Technology drawing No. 41703013A can be utilized for this task. The preferred embodiment of the support frame would consist of two square aluminum posts with gusseted base plates welded to the bottom of each post. A rigid torque tube would be pinned and bolted to the square posts beneath the wiggler assembly. The torque tube will prevent any adverse misalignment between the two posts and provide a more rigid assembly for transport and installation then does the current stand.

A six strut support system will be utilized to suspend the wiggler from the aluminum posts. Four struts shall form a dual parallel linkage system for role and yaw rigidity. It can be seen that this system is over constrained by one linkage. However, the rigidity of the current support column and frame system has been questioned and the use of one auxiliary strut to stiffen the frame is advised. Vertical support is performed by two struts that are attached between the aluminum support post and the adapter plates. The vertical support struts are located near the axial centroid of the wiggler assembly.

Two adjustment screws in the vertical aluminum posts control axial positioning. Detachable wheel sets will allow transport and installation of the wiggler assembly into the ATF experimental hall with benign or negligible consequences to the surrounding equipment. It is suggested that the proposed support frame be fabricated and mated to the Cornell wiggler at Argonne National Laboratory ANL. Field mapping and shimming for the poles of the Cornell wiggler shall be performed by ANL. Once completed, the assembly will be shipped to BNL.

The wiggler will be uncrated, inspected and presurveyed in Bldg. 726. A quick measurement of the magnet will be performed with either a scanning hall probe or the pulsed wire set-up. This data will be compared with that taken at Argonne to be sure that the magnet has not been damaged in transit or handling (shifting of shims for example). Once completed, the chamber assembly (described in the next section) will be mated to the wiggler stand and presurveyed to the magnetic center of the wiggler. The wiggler will then be transported to the ATF experimental hall.

The down beam spool pieces of beamlines 2 and 3 shall have been valved off, brought up to air and then temporarily removed for wiggler access. Beamline 2 shall have been modified by removal and repositioning of the IFEL experiment and relocation of the bunching detector. Partial removal of shielding block around the end of beamline 1 will be necessary to roll the wiggler assembly into position.

Half inch red heads shall be drilled into the floor using holes in the aluminum base plates as pilots. The weight of the wiggler shall be off loaded from the wheels on to threaded studs protruding from the red headed holes in the floor. The assembly shall be leveled and secured to the floor studs. The NSLS survey group shall utilize the fiducials, strut system, and the presurvey data to place the wiggler assembly on the desired beamline and lock the assembly into place. The area beneath the support posts shall be filled with grout.

Vacuum chamber and electron beam diagnostics

Overview:

The concept for the chamber to be utilized in the experiment is to adapt existing NISUS spares to the CHESS wiggler. Four Four-wire Steering/Focus chambers are to be included, with modified adapter pieces separating sections. The adapters are different than their NISUS equivalent. They are reduced in length, and have provision for mounting both the pumping and diagnostics from the same side of the chamber. This is required for integration with the chamber support described in the previous section. Pop-in monitors are to be provided at each end of the correctors, for a total of five monitors. The entire assembly is to be mounted from an aluminum jig plate, which is attached to the wiggler support via a six strut suspension.

Chamber:

The basic chamber is fabricated from aluminum extrusion developed for the NISUS undulator. The nominal chamber height through the gap of the undulator is 0.531" [13.5 mm]. In NISUS, the nominal specified minimum gap is 14.4 mm. The clear aperture of the chamber is 0.435" [11 mm]. The chamber sections and auxiliary ports are sealed with lead c-rings. We have built up a prototype chamber for testing and found, as did STI in their original work, that these seals function quite well, and that base pressures in the high 10^{-9} Torr range are readily achievable. In the ATF installation, the chamber will be clamped to a reference mounting plate, and shimmed from offset standards to provide the alignment. The plate will also be used as the mounting surface for the ancillary systems including pumps and diagnostic monitors.

Direct pumping will be provided by three 20 l/s ion pumps mounted on the plate. Two will serve two pump out ports each via a split manifold, while the odd remaining chamber has its own pump. Roughing valves and ion gauges will also be mounted on these manifolds as required.

Diagnostics:

Electron beam diagnostics will be provided by pop-in monitors. A coaxial actuator with precision location will be used for this application because access to the chamber is limited to only one side. The actuator will facilitate the use of either phosphor flags, YAG screens, or optical transition radiation (OTR) screens. For viewing the screens, COHU series 4910 monochrome CCD cameras will be used. They will each be fitted with a 2x converter and a Computar 55 Telecentric lens. This combination should provide imaging of the screen with spatial resolution the order of 10 micrometers. The light from the screen will be collected from the front surface of a right angle roof prism. This allows folding of the optical path to conserve space, and will allow us to illuminate the screen with a lamp through the back face of the prism for position and focus verification in the absence of electron beam.

These cameras can be gated, and can be configured to integrate signal in the CCD The images will be collected by the frame grabber for the ATF. Analysis of the intensity, position, and profile should be easily obtained in this manner.

Correctors:

The design principles for the Steering/Focus correctors have been fully described in the NISUS report. In terms of application, we note that in NISUS focusing is provided primarily by the canted poles. For this experiment, essentially all of the focusing must be supplied by the correctors.

For the parameters of the ATF accelerator and CHESS undulator, this will require a current of roughly 30A to supply the quadrupole focusing. Smaller currents of less than 10A should be adequate to provide the required steering corrections. To achieve this, we propose to connect all 16 of the wires in series and power them from a single 50A power supply. Smaller 'bleeder' supplies will be connected in parallel with each trim wire to allow adjustment of the current in each wire. Dipole corrections can then be imposed by coordination of the currents (and directions of currents) superimposed on each wire.

Control of these supplies will be coordinated with the ATF control system, requiring the allocation of 17 additional D/A channels. Algorithms for computing the currents required to provide steering kicks in each plane will be developed so that in operation, the user will only need to select the desired correction, the computer will then provide the appropriate signal to the required power supplies.

Seed laser injection

The ATF laser system consists of Nd:YAG and CO_2 lasers. The 1.06 μm, 10-ps, 1 GW Nd:YAG laser serves for picosecond slicing in the CO_2 laser system and, after frequency quadrupling, as a linac photocathode driver. The 10.6 μm, 100-ps, 10 GW CO_2 laser beam is transported to several locations in the experimental hall, where it interacts with e-bunches to test different laser accelerator schemes.

The diagram below shows main sub-components of the ATF laser system and illustrates joint operation of YAG and CO_2 lasers serving for the projected FEL experiment. Actively mode-locked CW YAG oscillator generates a train of 12-ns spaced 15-ps pulses of linearly polarized radiation at =1.06 μm, synchronized to a sub-harmonic of the linac RF field. A Pockels cell switch, in combination with a polarizer, cuts out single pulses in a 3 Hz sequence. After 4-pass preamplifier and double-pass amplifier, pulses acquire 20 mJ energy. Part of this energy is split to control picosecond slicing in the CO_2 laser system. Other portion is directed through the 2nd and then 4th harmonic crystals to a photocathode generating 12-ps electron bunches.

Application of a mode-locked laser as a RF gun driver puts strict requirements on the stability of all laser parameters. Such requirements are satisfied by using a diode-pumped laser oscillator that is characterized by appropriately small jitters in power and mode-lock timing. Also, we use relay imaging and spatial filtering throughout the system, with long portions of beam path enclosed in evacuated tubes.

The CO_2 laser delivers high-power pulses of IR radiation synchronized with the electron bunches. Such synchronization is automatically achieved by semiconductor optical switching of a several picosecond pulse out of a 100-ns 1-MW oscillator output using the same Nd:YAG laser pulse which is ultimately used to drive a photocathode. The YAG pulse, having photon energy above the band gap of a semiconductor (Ge), creates electron-hole plasma in a surface layer. When the plasma reaches critical density refractive index becomes imaginary, and Ge, which is normally transparent to 10-μm radiation, turns into a highly reflective mirror. After the control pulse termination, the drop of the reflectivity from the Ge has a characteristic time, which is that of diffusion of the free-carriers into the bulk material, ca. 150 ps. To define the trailing edge of the pulse, shortening it to a few picoseconds, transmission switching, the complement to reflection switching is used for the second stage. Using the same fast laser initiator for the linac and CO_2 laser ensures the desired picosecond synchronization of the electron bunch and laser pulse at their interaction point.

The sliced pulse is transmitted through the 3-atm, UV-pre-ionized, 120-cm long amplifier energized by a 150-kV pulsed discharge. The first four passes are arranged in a double-X configuration using a 4-mirror set-up. To increase the total gain to ~10^5, the beam is redirected for the next 4 passes through the amplifier. The active Pockels optical isolator, in combination with a passive plasma shutter, prevents parasitic self-lasing, otherwise inevitable in such a scheme.

Ultimately, after 8 passes through the amplifier we measure 1 J output energy in a 100-ps pulse, which corresponds to the spectral-bandwidth-limited minimum pulse duration sustained by the 3-atm CO2 amplifier. Amplified to 10 GW peak power, the CO_2 laser pulses are transported to the experimental hall where they are used for various experiments. In particular, the laser beam has been introduced into Beam Line 2 and used successfully in the Inverse Free-Electron Laser experiment. The IFEL is in many respects similar to a single pass FEL amplifier thus the ATF has the necessary experience and equipment for injecting a seed laser pulse to the Cornell wiggler at Beam Line 2.

CO_2 Laser parameters	UNITS	VALUE
Oscillator Peak Power	MW	1
Oscillator Pulse Duration	ns	100
Switched Pulse Duration	ps	~300
Double Sliced Pulse Duration	ps	10-300
Amplified Pulse Duration	ps	100
Output Energy	J	1
Output Peak Power	GW	10
Repetition Rate	Hz	0.1